



OPEN Co-delivery of NGF and BMP-2 via thermosensitive pluronic F127 hydrogel enhances chondrogenesis and cartilage repair

Yue Huang^{1,2,3,4}, Bin Shi^{1,2,3}✉, Yongyang Liao^{1,2,3}, Gengsen Zou^{1,2,3} & Kun Song^{1,2,3}

Cartilage defects are difficult to repair due to the tissue's avascular nature, low cell density, and limited regenerative capacity. Growth factor-based tissue engineering offers a promising strategy for enhancing cartilage regeneration. This study aimed to develop a synergistic and sustained dual-growth factor delivery system by co-loading nerve growth factor (NGF) and bone morphogenetic protein-2 (BMP-2) into a Pluronic-F127 hydrogel, and to investigate its effects and underlying mechanisms in promoting chondrocyte regeneration and mesenchymal stem cell chondrogenesis. A thermosensitive Pluronic-F127 hydrogel was prepared to encapsulate NGF and BMP-2. The loading efficiency and release kinetics of both growth factors were quantified. In vitro experiments were conducted to assess cell proliferation, migration, and differentiation using CCK-8 assays, scratch tests, RT-qPCR, Western blotting, and matrix synthesis assays in human chondrocytes and bone marrow-derived mesenchymal stem cells (hBMSCs). The NGF/BMP-2@Pluronic-F127 hydrogel demonstrated high loading efficiency and sustained release of both factors. Co-delivery significantly enhanced proliferation and migration of chondrocytes and hBMSCs compared to single-factor or control treatments. Expression of chondrogenic markers (COL2A1, AGG, SOX9) was markedly upregulated at both mRNA and protein levels. Additionally, the hydrogel promoted glycosaminoglycan and DNA synthesis, indicating enhanced matrix production and cellular activity. These findings support a synergistic mechanism in which NGF improves cell viability and modulates the microenvironment, while BMP-2 activates chondrogenic signaling pathways to induce differentiation. The NGF/BMP-2@Pluronic-F127 co-delivery system offers a promising strategy for cartilage regeneration by integrating proliferative, migratory, and chondrogenic cues within a single hydrogel platform. This approach may help overcome the limitations of current treatments and improve outcomes in condylar cartilage defect repair.

Keywords BMP-2, Cartilage repair, Tissue engineering, Hydrogel, NGF

Cartilage defects, caused by trauma, degenerative diseases like osteoarthritis, inflammation, or genetic disorders, pose significant challenges due to the limited self-repair capacity of cartilage tissue. This is primarily attributed to the avascular nature, low cell density, and restricted nerve distribution in cartilage, which impair its ability to regenerate^{1,2}. While traditional treatments, such as anti-inflammatory medications, microfracture surgery, and osteochondral transplantation, offer symptom relief or temporary repair, they are associated with issues like the formation of mechanically inferior fibrocartilage and donor tissue scarcity. These limitations underscore the urgent need for innovative strategies in cartilage repair^{3–8}.

Cartilage tissue engineering holds significant promise for cartilage repair. Using engineered scaffolds, seed cells, and growth factors, this approach can effectively promote cartilage regeneration⁹. Tissue engineering recreates a cartilage-like microenvironment by combining scaffolds for structural support, seed cells capable of chondrogenic differentiation, and growth factors that regulate cell proliferation and matrix synthesis^{10,11}. Hydrogels are widely employed as scaffolds due to their high water content, biocompatibility, and injectability,

¹Department of Oral and Maxillofacial Surgery, First Affiliated Hospital of Fujian Medical University, No. 20 Cha Zhong Road, Fu'an City 350005, Fujian Province, China. ²Department of Oral and Maxillofacial Surgery, National Regional Medical Center, Binhai Campus of the First Affiliated Hospital, Fujian Medical University, No. 999 Huashan Road, Fuzhou City 350212, Fujian Province, China. ³School and Hospital of Stomatology, Fujian Medical University, No. 246 Yanqiao Middle Road, Fuzhou City 350004, Fujian Province, China. ⁴Laboratory of Facial Plastic and Reconstruction, Fujian Medical University, Fuzhou, China. ✉email: drshibin@163.com

providing a favorable environment for chondrocyte activity^{12,13}. Among them, Pluronic-F127, a thermosensitive copolymer, undergoes sol–gel transition at physiological temperature, enabling minimally invasive administration and sustained release of embedded factors¹⁴. Controlling the hydrogel's degradation rate enables sustained release of drugs and growth factors, promoting cartilage regeneration. This controlled release can enhance the bioavailability of therapeutic agents, improving their efficacy and reducing the frequency of administration¹⁵.

Bone morphogenetic protein 2 (BMP-2) plays a crucial role in cartilage repair. This multifunctional growth factor enhances the differentiation and proliferation of osteoblasts and chondrocytes, boosting the regenerative capacity of cartilage tissue¹⁶. BMP-2 promotes cartilage regeneration by activating signaling pathways (e.g., Smad) that enhance chondrocyte proliferation, survival, and matrix synthesis, including type II collagen and proteoglycans^{17–19}. Despite its promising effects, the clinical application of BMP-2 faces challenges like rapid diffusion and degradation, necessitating the development of appropriate carrier systems for sustained release. Researchers have developed various carrier systems, including biodegradable hydrogels and microspheres, to enhance BMP-2 efficacy in cartilage repair. These carriers can protect BMP-2 from premature degradation and facilitate its localized delivery to the defect site^{20–23}.

Nerve growth factor (NGF) significantly contributes to cartilage repair. NGF is essential for nerve growth and regeneration and promotes angiogenesis and the proliferation and migration of bone tissue cells. These properties make NGF a valuable bioactive factor for cartilage repair^{24–26}. Clinically, NGF is often combined with other growth factors to improve therapeutic outcomes. For instance, the combination of NGF and BMP-2 significantly enhances cartilage repair^{27,28}. Researchers have developed various sustained release systems for NGF to maximize its efficacy in vivo²⁹.

In this study, we designed a Pluronic-F127 hydrogel co-loaded with NGF and BMP-2 to explore its application and mechanisms in repairing condylar cartilage defects. By combining NGF and BMP-2 in the Pluronic-F127 hydrogel, we aim to leverage their synergistic effects to optimize cartilage repair. The combination of these growth factors in a temperature-sensitive hydrogel could provide a sustained and localized release, enhancing the regenerative capacity of the cartilage tissue.

Materials and methods

Materials

NGF was purchased from Wuhan Pulunsi Life Science and Technology Co., Ltd. Bone Morphogenetic Protein-2 (BMP-2) was acquired from MedChemExpress. Pluronic F-127 was obtained from Biyun Tian Biotech. All other reagents were procured from Maclin Biochemical Corporation. Unless otherwise specified, all the chemicals used in the experiments were of reagent grade and were used without further purification.

Preparation of hydrogels

Pluronic-F127 was dissolved in distilled water to prepare a 15% (w/v) Pluronic-F127 solution. BMP-2 and NGF were then added to the Pluronic-F127 solution to achieve a final concentration of 2 ng/mL for each growth factor, i.e., 2 ng of BMP-2 and 2 ng of NGF per mL of Pluronic-F127 solution. The prepared solution was stored at 4 °C for future use.

Loading efficiency and in vitro release study of NGF and BMP-2

The loading efficiency of NGF and BMP-2 in the Pluronic-F127 hydrogel was determined by quantifying the unencapsulated growth factors in the supernatant. After hydrogel preparation, samples were centrifuged at 12,000 rpm for 10 min to separate the gel from the unbound solution. The concentrations of free NGF and BMP-2 in the supernatant were measured using commercial ELISA kits. The loading efficiency (%) was calculated using the following formula:

$$\text{Loading efficiency (\%)} = [(\text{Total amount} - \text{Free amount}) / \text{Total amount}] \times 100\%.$$

Subsequently, the in vitro release behavior of NGF and BMP-2 from the hydrogel was evaluated using a dialysis method. Briefly, 500 µL of hydrogel was placed into a dialysis bag (molecular weight cutoff: 8–14 kDa) and immersed in 10 mL of PBS (pH 7.4) containing 0.1% BSA, maintained at 37 °C under gentle shaking. At appropriate time intervals, aliquots of the release medium were collected and replaced with fresh PBS to maintain sink conditions.

The concentrations of BMP-2 and NGF in the collected samples were measured using ELISA kits: Human BMP-2 ELISA Kit (PB045, Beyotime, China) and Human NGF ELISA Kit (COIBO BIO, China). Cumulative release percentages were calculated based on standard curves to evaluate the sustained release performance of the hydrogel system.

Cell culture and experimental grouping

Chondrocytes (CP-H107) and human bone marrow-derived mesenchymal stem cells (hBMSCs, CP-H166) were purchased from Wuhan Procell Life Science & Technology Co., Ltd. Cells were cultured in their respective complete media (Human Chondrocyte Complete Culture Medium (CM-H107) and Mesenchymal Stem Cell Complete Medium (CM-H166), Procell, Wuhan, China), supplemented with 10% fetal bovine serum (FBS) and 100 U/mL penicillin-streptomycin, at 37 °C in a humidified atmosphere containing 5% CO₂. Upon reaching 80–90% confluence, cells were trypsinized using 0.25% trypsin-0.02% EDTA solution and neutralized with complete medium. The cells were then centrifuged at 800 rpm for 5 min at 4 °C, and the pellet was resuspended in fresh medium for further passaging or plating. For experimental grouping, cells were divided into the following groups:

Control: Normal culture conditions without treatment.

BMP-2@Pluronic-F127: Cells treated with BMP-2 encapsulated in Pluronic-F127.

NGF@Pluronic-F127: Cells treated with NGF encapsulated in Pluronic-F127.

NGF/BMP-2@Pluronic-F127: Cells treated with a co-delivery system of NGF and BMP-2 in Pluronic-F127.

CCK-8 assay for cell proliferation

Chondrocytes and hBMSCs were seeded in 96-well plates at a density of 1500 cells per well and allowed to adhere for 24 h, respectively. Following this incubation period, various experimental samples were added to the respective wells. After a further 24 h of co-cultivation with the cells, 10 μ L of CCK-8 solution was added to each well, and the plates were incubated for an additional 2 h before the end of the experiment. Cell viability and proliferation were assessed by measuring the absorbance at OD450 using a microplate reader (Thermo Fisher, USA). Meanwhile, the cell morphology and proliferation status of both chondrocytes and hBMSCs were observed at 0, 24, and 48 h using an inverted phase-contrast microscope (Leica DMi1, Germany) and representative images were recorded to qualitatively assess growth behavior under different treatments. Each treatment group was tested in triplicate ($n=3$) across three independent experiments.

Scratch assay for cell migration

Chondrocytes were digested with 0.25% trypsin, suspended, and adjusted to a density of 1×10^5 cells/mL. They were then seeded into 6-well plates and cultured with hydrogel solutions in serum-free medium until 90% confluence was reached. After a 24-hour serum starvation, scratches were made using a 10 μ L pipette tip, creating parallel wounds. Detached cells were removed with PBS washes, and fresh serum-free medium was added. Images of the scratches were captured at 0 h and after 24 h of culture to assess cell migration by measuring the wound closure via microscope (Shanghai Optical Instrument, China). The scratch assay was performed in triplicate ($n=3$) and repeated in three independent experiments.

RT-qPCR

Total RNA was extracted from cells using a specific kit, and the concentration and purity were determined using a Nano 600 instrument. For cDNA synthesis, 500 ng of RNA was reverse-transcribed using a high-capacity cDNA reverse transcription kit. Real-time quantitative PCR was performed using specific primers for collagen type II alpha-1 gene (COL2A1), aggrecan (AGG), SRY-related protein 9 (SOX9), and GAPDH. The reactions were carried out in a CFX96 Touch real-time PCR system (Bio-Rad, USA), and relative gene expression was calculated using the $2^{-\Delta\Delta C_t}$ method. Gene expression analysis was conducted with triplicate samples ($n=3$) from three independent experiments. The sequence of mRNA is shown in Table 1.

Western blot analysis

Total cellular protein was extracted from hBMSCs in the logarithmic growth phase, which were plated in 6-well plates and treated according to the experimental groups. Protein concentrations were quantified using the bicinchoninic acid (BCA) assay kit (P0009, Beyotime, Shanghai, China), following the manufacturer's protocol and the method originally described by Smith et al. (1985)³⁰. Equal amounts of protein were loaded onto a 12% separating gel and 5% stacking gel for SDS-PAGE. After electrophoresis, proteins were transferred onto a PVDF membrane, blocked, and incubated with primary antibodies overnight at 4 $^{\circ}$ C. After washing, the membrane was incubated with the appropriate secondary antibodies for 2 h at room temperature. Protein expression was visualized by JP-K600 chemiluminescence imaging system (Shanghai Jiapeng, China), and band densities were analyzed using Image J software (1.8.0). Protein expression was assessed using triplicate samples ($n=3$) from three independent experiments.

Investigation of the effects of various hydrogels on chondrocyte DNA and glycosaminoglycan (GAG) synthesis

Sample treatment and co-culture with cells

5×10^5 chondrocytes were seeded in each well of a 6-well plate. After 24 h, the medium was replaced with complete culture medium containing 100 mg/mL of each group's extract solution, with DMEM/F12 complete culture medium serving as the control group. The cells were fed every other day, and after 7 days of culture, they were washed with PBS solution. Then, 1 mL of papain digestion solution was added to each well, and the plate was placed in a 65 $^{\circ}$ C constant temperature shaker for 16 h of digestion. After centrifugation, the supernatant was collected.

Gene	The sequences of the mRNA primers
COL2A1	Forward: GCTCCTGCCGTTTCGCTG
	Reverse: ATTATACCTCTGCCCATCCTGC
AGC	Forward: CGTGTAAAAAGGGCACAGCC
	Reverse: GGAAGCTCTTCTCAGTGGGC
SOX9	Forward: CAAGAAGGACCACCCGATT
	Reverse: AAGATGGCGTTGGGGGAGAT
GAPDH	Forward: AATGGGCAGCCGTTAGGAAA
	Reverse: GCGCCCAATACGACCAAATC

Table 1. The sequence of mRNA.

Quantitative detection of DNA in samples

The Hoechst 33,258 assay was used to measure the total DNA content in chondrocytes from different samples³¹. First, 100 μ L of the papain-digested samples was taken and added to a 96-well culture plate, followed by the addition of 100 μ L of Hoechst 33,258 solution (1 μ g/mL) to each well. The mixture was incubated at room temperature in the dark for 5 min to allow for full reaction. Then, the OD values of each group were measured using a fluorescence plate reader (Thermo Fisher, USA) at an excitation wavelength of 355 nm and an absorption wavelength of 460 nm. A standard curve was plotted using calf thymus DNA as the standard (standard stock solution 1 mg/mL in H₂O; standard curve concentrations: 0, 15.625, 31.25, 62.5, 125, 250, 500, 1000 pg/mL).

Quantitative detection of GAG in samples

The 1,9-dimethylmethylene blue (DMMB) assay was used to measure the GAG content in different samples³². First, 40 μ L of the papain-digested samples was taken and added to a 96-well culture plate, followed by the addition of 125 μ L of DMMB solution (10.5 g DMMB was fully dissolved in a 5 mL anhydrous ethanol solution containing 1.0 g of sodium acetate, then brought to a final volume of 400 mL with distilled water, adjusted to a pH of 3.5 with a sodium acetate solution, and finally brought to a final volume of 500 mL, stored at room temperature in the dark) to each well. The plate was gently shaken to ensure thorough mixing and reaction; the OD values of each group were measured using a plate reader (Thermo Fisher, USA) at 595 nm. A standard curve was plotted using chondroitin sulfate as the standard (standard stock solution 500 μ g/mL in H₂O; standard curve concentrations: 0, 1.25, 2.5, 5, 7.5, 10 μ g/mL). The quantification of GAG and DNA synthesis was performed in triplicate ($n=3$) and repeated in three independent experiments.

Data analysis

Data were analyzed using GraphPad Prism 9 (Version 9.4.0) for statistical analysis and graphing. All data are presented as means \pm SD, $n=3$. Statistical differences between groups were assessed using T-Test or One-way ANOVA, with a P-value of less than 0.05 considered statistically significant.

Results

Loading efficiency and in vitro release profiles of growth factors

The loading efficiencies of BMP-2 and NGF in the Pluronic-F127 hydrogel were calculated based on the concentrations of unencapsulated growth factors in the supernatant after gel formation. The loading efficiency was found to be approximately $86.3\% \pm 2.8\%$ for NGF and $74.1\% \pm 3.2\%$ for BMP-2, indicating that both growth factors were efficiently incorporated into the hydrogel network.

The in vitro release profiles of BMP-2 and NGF over 48 h showed a sustained and gradual release behavior (Fig. 1A–B). During the initial release phase, a mild burst release was observed, followed by a stable release phase. At 48 h, the cumulative release reached $65.92 \pm 3.75\%$ for NGF and $80.4\% \pm 3.97$ for BMP-2, respectively. These results demonstrate that the Pluronic-F127 hydrogel system enables effective loading and controlled release of growth factors, ensuring their sustained bioavailability at the target site, which is critical for supporting cartilage tissue repair.

Chondrocyte and hBMSCs cell proliferation

The assessment of cell proliferation using the CCK-8 assay unveiled pronounced effects of the co-delivery system on both chondrocyte and hBMSCs proliferation. Specifically, for chondrocytes, the NGF/BMP-2@Pluronic-F127 group exhibited a marked increase in cell viability at both 24 and 48 h, with OD450 values reaching 4.394 and 6.036, respectively. These values were significantly higher compared to the BMP-2@Pluronic-F127 group, which showed OD450 values of 3.831 at 24 h and 5.370 at 48 h, and the NGF@Pluronic-F127 group, with OD450 values of 3.959 at 24 h and 5.26 at 48 h (Fig. 2A). This indicates a superior proliferative effect of the combined

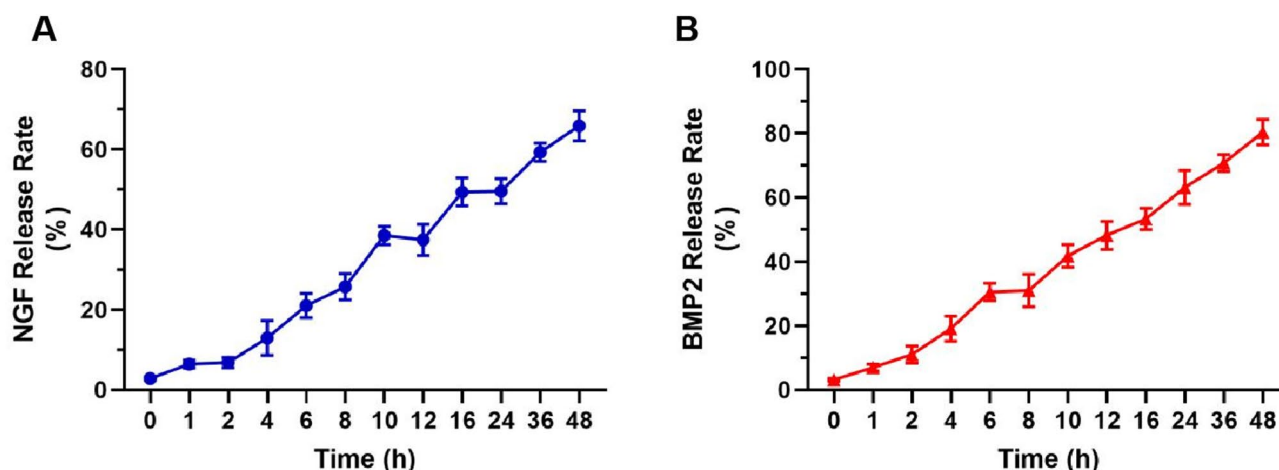


Fig. 1. In vitro release profiles of NGF (A) and BMP-2 (B) over 48 h. Data are presented as mean \pm SD ($n=3$).

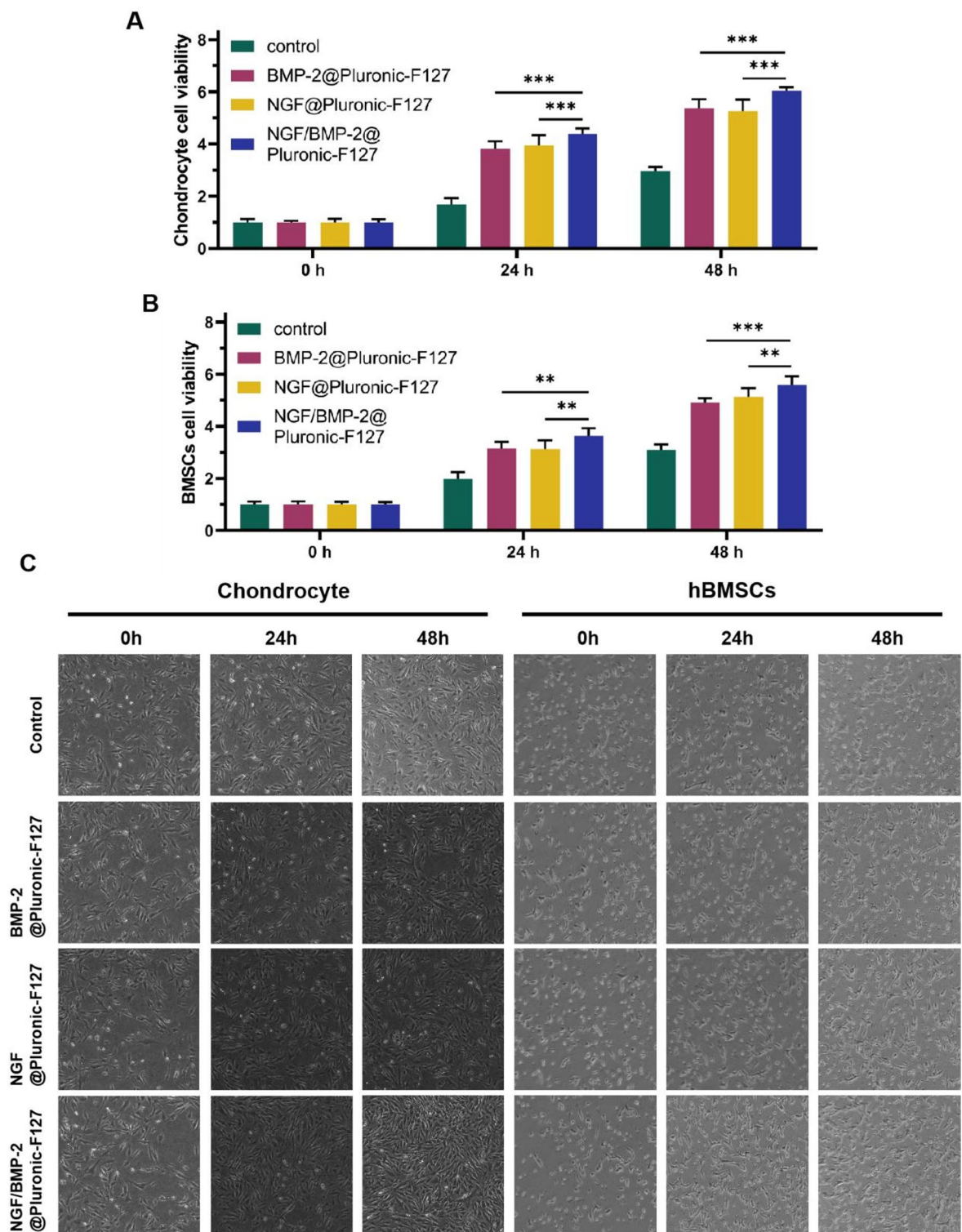


Fig. 2. Chondrocyte and hBMSCs Cell Proliferation detected by CCK-8 assay, (A) CCK-8 assay measured the cell proliferation of chondrocytes in each group after 24 h and 48 h of co-culture; (B) CCK-8 assay measured the cell proliferation of hBMSCs in each group after 24 h and 48 h of co-culture; (C) Microscopy images of chondrocytes and hBMSCs were taken at 24 and 48 h after treatment. Control: Normal culture conditions without treatment, BMP-2@Pluronic-F127: Cells treated with BMP-2 encapsulated in Pluronic-F127, NGF@Pluronic-F127: Cells treated with NGF encapsulated in Pluronic-F127, NGF/BMP-2@Pluronic-F127: Cells treated with a co-delivery system of NGF and BMP-2 in Pluronic-F127, **($p < 0.01$), ***($p < 0.001$) ($n = 3$).

growth factors compared to individual treatments. In the case of hBMSCs, the NGF/BMP-2@Pluronic-F127 group similarly demonstrated a robust proliferation rate, with OD450 values of 3.63 at 24 h and 5.99 at 48 h. These values were notably higher than those of the BMP-2@Pluronic-F127 group, which had OD450 values of 3.149 at 24 h and 4.911 at 48 h, and the NGF@Pluronic-F127 group, with OD450 values of 3.133 at 24 h and 5.143 at 48 h (Fig. 2B).

The superior cell viability and proliferation rates in the NGF/BMP-2@Pluronic-F127 group for both chondrocytes and hBMSCs suggest that the co-delivery system provides a more conducive environment for cell growth and division. This enhanced proliferation is a critical factor for the rapid healing of cartilage defects, as it facilitates the filling of the defect site with newly formed cells and the subsequent deposition of extracellular matrix components. To further support these findings, phase-contrast microscopy images of chondrocytes and hBMSCs were taken at 24 and 48 h after treatment to observe morphological changes (Fig. 2C). In the NGF/BMP-2@Pluronic-F127 group, cells exhibited significantly higher density and a more compact arrangement compared to the control and single-factor groups. hBMSCs in this group gradually transitioned from a spindle-shaped morphology to round or oval shapes and tended to form small aggregates. In addition, translucent matrix-like material was occasionally observed in the extracellular space, suggesting early signs of cartilage matrix secretion.

Enhancement of chondrocyte migration

The migratory capacity of chondrocytes, a key parameter for cartilage repair, was assessed using the scratch assay. The results demonstrated a significant enhancement in the healing rate for the NGF/BMP-2@Pluronic-F127 group after a 24-hour period, achieving a remarkable healing rate of 80.01%. This value is substantially higher than that of the control group, which exhibited a healing rate of 36.65% (Fig. 3A–B). The pronounced difference in healing rates between the NGF/BMP-2@Pluronic-F127 group and the control group indicate that the co-delivery system has a potent effect on promoting chondrocyte migration. This acceleration of cell migration is crucial for the rapid repopulation of damaged areas within the cartilage, facilitating the initiation of tissue repair processes. The enhanced migration observed in the NGF/BMP-2@Pluronic-F127 group may be attributed to

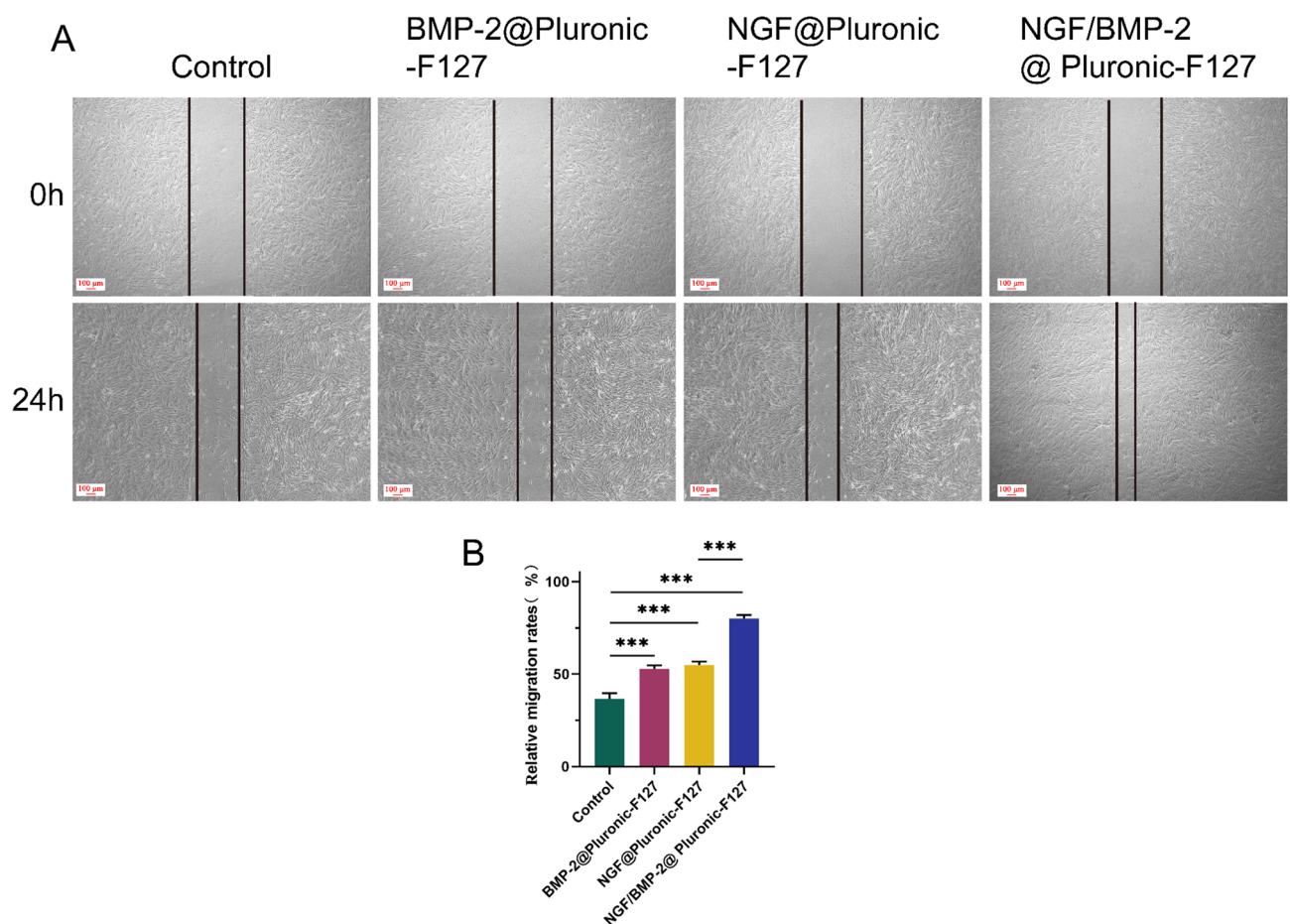


Fig. 3. Chondrocyte Migration assessed by scratch assay, (A) Scratch test results of each group and chondrocytes cultured for 0 h and 24 h, and (B) quantitative analysis of cell mobility. Control: Normal culture conditions without treatment, BMP-2@Pluronic-F127: Cells treated with BMP-2 encapsulated in Pluronic-F127, NGF@Pluronic-F127: Cells treated with NGF encapsulated in Pluronic-F127, NGF/BMP-2@Pluronic-F127: Cells treated with a co-delivery system of NGF and BMP-2 in Pluronic-F127, **($p < 0.01$), ***($p < 0.001$) ($n = 3$).

the synergistic action of BMP-2 and NGF, which are known to influence cell motility and extracellular matrix remodeling. The BMP-2@Pluronic-F127 and NGF@Pluronic-F127 groups also showed increased healing rates of 52.85% and 54.88%, respectively, suggesting a positive effect of each growth factor individually, yet highlighting the superiority of their combination.

Differentiation of hBMSCs into chondrocytes

The differentiation of hBMSCs into chondrocytes was evaluated through the quantification of specific chondrogenic markers by RT-qPCR. The expression levels of COL II, AGG, and SOX9 were significantly higher in the NGF/BMP-2@Pluronic-F127 group compared to the control group. The $2^{-\Delta\Delta CT}$ values indicated approximately a 2.82-fold increase for COL II and a 3.87-fold increase for AGG in the NGF/BMP-2@Pluronic-F127 group (Fig. 4A–B). Additionally, the SOX9 gene, a master regulator of chondrogenesis, showed an upregulation of approximately 3.65-fold, suggesting that the co-delivery system significantly enhances the chondrogenic potential of hBMSCs (Fig. 4C). The Western blot analysis further corroborated these findings, demonstrating enhanced protein expression of COL2a1 and AGG in the NGF/BMP-2@Pluronic-F127 group. Specifically, the COL2a1 protein expression was 2.18 times higher, and the AGG protein expression was 1.88 times higher than that of the control group (Fig. 5A–B). These results collectively demonstrate that the NGF/BMP-2@Pluronic-F127 system is effective in inducing the differentiation of hBMSCs into chondrocytes, highlighting its potential as a promising therapeutic approach for cartilage regeneration.

Enhancement of GAG synthesis

The results from the quantification of GAG synthesis revealed a significant increase in the production of this critical cartilage matrix component in response to the treatment with BMP-2@Pluronic-F127 and NGF@Pluronic-F127, as compared to the control group. Specifically, the BMP-2@Pluronic-F127 and NGF@Pluronic-F127 groups exhibited GAG synthesis levels of 3.7 ± 0.34 μ g/mL and 3.81 ± 0.3 μ g/mL, respectively. Notably, the NGF/BMP-2@Pluronic-F127 group demonstrated a substantially higher GAG synthesis level of 5.05 ± 0.28 μ g/mL (Fig. 6A–B). This substantial increase in GAG synthesis indicates that the co-delivery system is effective in promoting the production of a fundamental component of the cartilage matrix.

Furthermore, the assessment of chondrocyte DNA synthesis yielded compelling results, with the NGF/BMP-2@Pluronic-F127 group showing a marked increase, reaching 81.69 ± 8.45 pg/mL, which is approximately 2.25 times that of the control group. This increase was also significantly higher compared to the BMP-2@Pluronic-F127 and NGF@Pluronic-F127 groups. These findings reflect the proliferative effect of the combined growth factors within the NGF/BMP-2@Pluronic-F127 system on cells within the cartilage microenvironment.

The heightened DNA synthesis, in conjunction with the elevated GAG content, underscores the capacity of NGF/BMP-2@Pluronic-F127 to stimulate both the cellular proliferation and the biosynthetic activity of chondrocytes. These processes are pivotal for the repair and regeneration of cartilage. The collective upregulation of GAG synthesis and chondrocyte DNA synthesis by the NGF/BMP-2@Pluronic-F127 system highlights its dual role in fostering the cellular constituents and matrix production within the cartilage.

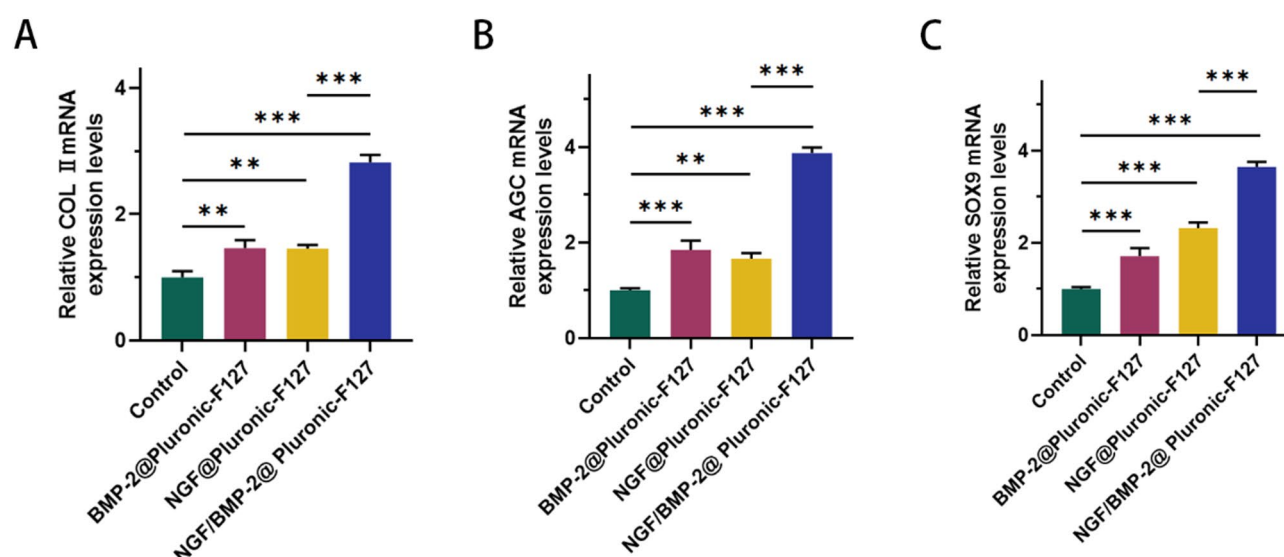


Fig. 4. mRNA expression level was detected by RT-qPCR, Control: Normal culture conditions without treatment, BMP-2@Pluronic-F127: Cells treated with BMP-2 encapsulated in Pluronic-F127, NGF@Pluronic-F127: Cells treated with NGF encapsulated in Pluronic-F127, NGF/BMP-2@Pluronic-F127: Cells treated with a co-delivery system of NGF and BMP-2 in Pluronic-F127, **($p < 0.01$), ***($p < 0.001$) ($n = 3$).

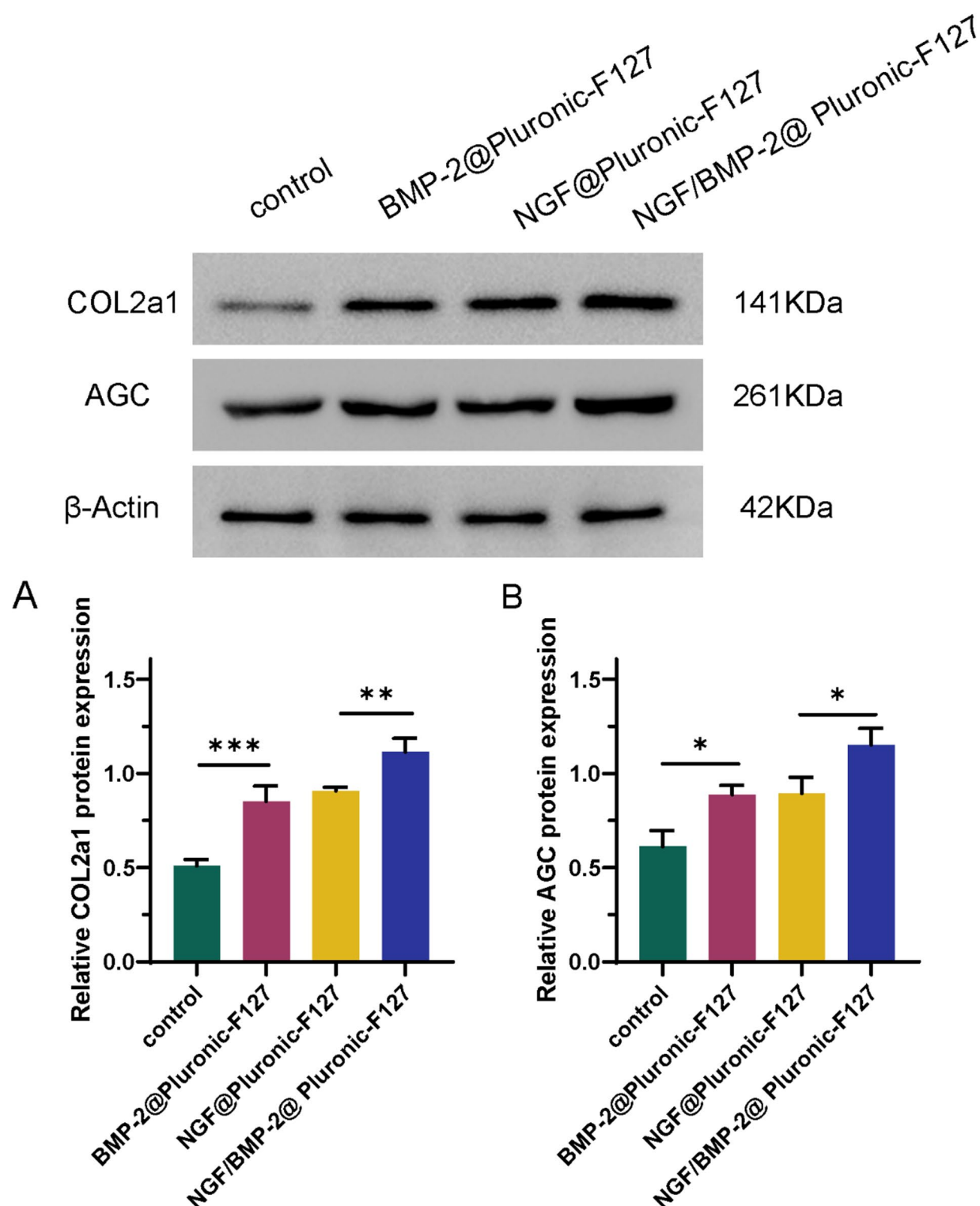


Fig. 5. Protein expression level was detected by WB, Control: Normal culture conditions without treatment, BMP-2@Pluronic-F127: Cells treated with BMP-2 encapsulated in Pluronic-F127, NGF@Pluronic-F127: Cells treated with NGF encapsulated in Pluronic-F127, NGF/BMP-2@Pluronic-F127: Cells treated with a co-delivery system of NGF and BMP-2 in Pluronic-F127, * ($p < 0.05$), ** ($p < 0.01$), *** ($p < 0.001$) ($n = 3$).

Discussion

Cartilage defects remain a major clinical challenge due to the tissue's limited self-repair capacity and the lack of effective long-term regenerative treatments. This study introduces a novel therapeutic strategy for cartilage defect repair using a Pluronic-F127 hydrogel co-loaded with NGF and BMP-2. This dual-growth factor delivery

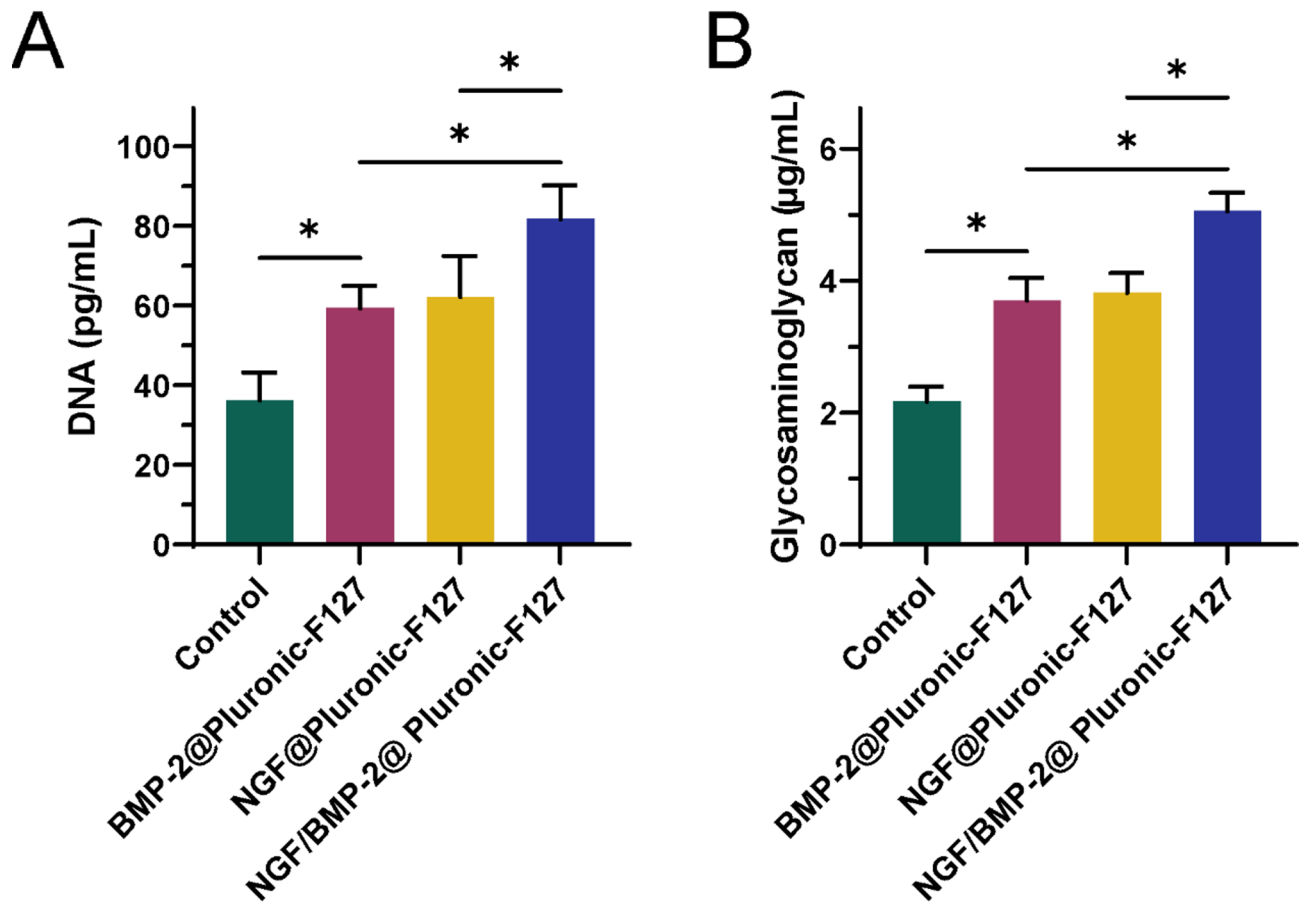


Fig. 6. The content of DNA and Glycosaminoglycan, Control: Normal culture conditions without treatment, BMP-2@Pluronic-F127: Cells treated with BMP-2 encapsulated in Pluronic-F127, NGF@Pluronic-F127: Cells treated with NGF encapsulated in Pluronic-F127, NGF/BMP-2@Pluronic-F127: Cells treated with a co-delivery system of NGF and BMP-2 in Pluronic-F127, **($p < 0.01$), ***($p < 0.001$), *($p < 0.05$) ($n = 3$).

system significantly enhances the proliferation, migration of chondrocytes and differentiation of hBMSCs into chondrocytes, as well as increases GAG synthesis, which are critical for the formation of cartilage matrix.

Pluronic-F127 was selected as a thermosensitive carrier due to its established biocompatibility and well-documented utility in drug and factor delivery. García-Couce et al. (2022) demonstrated that Pluronic-F127-based hydrogels are non-cytotoxic to human chondrocytes and can prolong intra-articular drug retention without exerting direct cellular effects³³. Furthermore, Guo et al. (2024) reported that PF127-hydrogel loaded with extracellular vesicles from adipose-derived mesenchymal stem cells (PF127-hydrogel@AMSC-EVs) promoted tracheal cartilage regeneration by enhancing delivery of the osteogenic regulator SCNN1B, while the hydrogel itself remained biologically inert³⁴. Consistent with these findings, our results suggest that the observed regenerative effects in cartilage are attributed to the biological functions of NGF and BMP-2 rather than the carrier itself. These findings underscore the importance of selecting delivery platforms that are bioinert yet effective in supporting the local action of therapeutic agents.

Our findings align with those reported by Rivera et al.²⁷ who demonstrated that local injections of β -NGF accelerate endochondral fracture repair by promoting the conversion of cartilage to bone. This provides a mechanistic understanding of how NGF can facilitate bone repair, which is relevant to our observations of enhanced chondrogenic differentiation and GAG synthesis in the presence of NGF. The use of Pluronic-F127 hydrogel as a scaffold for cell encapsulation and growth factor delivery has been well-recognized in tissue engineering. Our study builds upon this by demonstrating the synergistic effects of NGF and BMP-2 when co-delivered via the Pluronic-F127 hydrogel system. This synergy is particularly evident in the superior proliferation rates and chondrogenic differentiation of hBMSCs, which are key processes for cartilage regeneration, as highlighted by Wong et al.³⁵ in their discussion on the regulation of the microenvironment during endochondral repair.

The migratory capacity of chondrocytes, assessed through the scratch assay in our study, is a critical parameter for effective cartilage repair. Our results show a significant enhancement in the healing rate for the NGF/BMP-2@Pluronic-F127 group, consistent with the principles of spatiotemporal delivery of growth factors within bio-scaffolds, as discussed by Chen et al.³⁶. Notably, we also observed simultaneous increases in cell proliferation and chondrogenic differentiation in the same group. Although these processes are conventionally

regarded as temporally distinct or even opposing, increasing evidence suggests that in appropriately engineered microenvironments, particularly those involving sustained dual-factor delivery, these cellular responses can overlap³⁷. NGF has been reported to enhance extracellular matrix synthesis in chondrocytes through activation of the PI3K/AKT signaling pathway, suggesting a protective and pro-anabolic role in cartilage biology³⁸. BMP-2 has been shown to rapidly induce chondrogenic gene expression in BMSCs, even with short-term exposure, supporting its potent and temporally efficient role in driving early chondrogenesis³⁹. The localized and sustained release provided by the thermosensitive Pluronic-F127 hydrogel may contribute to the temporal convergence of these biological events. Furthermore, the inherent heterogeneity of chondrocytes and hBMSCs allows for coexisting subpopulations undergoing proliferation, migration, or early differentiation, depending on their intrinsic state and local signaling cues.

Furthermore, the observed enhancement of GAG synthesis and chondrocyte DNA synthesis by the NGF/BMP-2@Pluronic-F127 system underscores its potential to stimulate both cellular proliferation and the biosynthetic activity of chondrocytes. These processes are pivotal for cartilage repair and regeneration, as noted in reviews on advanced hydrogels for cartilage repair, which emphasize the need for materials that support the complex biological processes involved in tissue regeneration⁴⁰. Although NGF alone does not induce robust chondrogenic differentiation, it plays an important indirect role by enhancing the local microenvironment. NGF promotes cell survival, proliferation, and migration, while modulating inflammation and facilitating nutrient supply through mild angiogenesis. When co-delivered with BMP-2, NGF significantly amplifies BMP-2-driven chondrogenesis, consistent with our results and previous reports. In addition, the controlled and localized release of both factors from the Pluronic-F127 hydrogel reduces the risk of NGF-induced hypertrophy by limiting excessive angiogenesis. These findings suggest that NGF functions as a synergistic and supportive modulator, rather than a direct chondrogenic inducer, in the cartilage regeneration process.

In conclusion, our study provides insights into the synergistic effects of NGF and BMP-2 when co-delivered via a Pluronic-F127 hydrogel system for cartilage defect repair. BMP-2 activates Smad-dependent pathways to promote chondrogenic differentiation, while NGF enhances cell survival, migration, matrix synthesis, and modulates the inflammatory microenvironment, contributing to a more supportive regenerative niche. The co-delivery system enables sustained and spatially controlled release of both growth factors, better mimicking the natural gradients present during cartilage development and repair (Fig. 7). This strategy offers several translational advantages. Sustained release may reduce the dosage of BMP-2 required, minimizing its rapid degradation and potential side effects. Moreover, NGF's additional neurotrophic and angiogenic effects may further support tissue integration, nerve regeneration, and pain modulation. Importantly, this approach has the potential to promote the formation of hyaline cartilage rather than fibrocartilage, addressing a key limitation of current treatments such as microfracture or autologous chondrocyte implantation.

Conclusion

This study demonstrates the potent synergistic effects of the NGF/BMP-2@Pluronic-F127 co-delivery system on enhancing chondrocyte proliferation, migration, and the differentiation of hBMSCs into chondrocytes. The system's ability to significantly increase cell viability, accelerate tissue regeneration, upregulate chondrogenic gene expression, and stimulate GAG synthesis underscores its potential in advancing cartilage repair strategies.

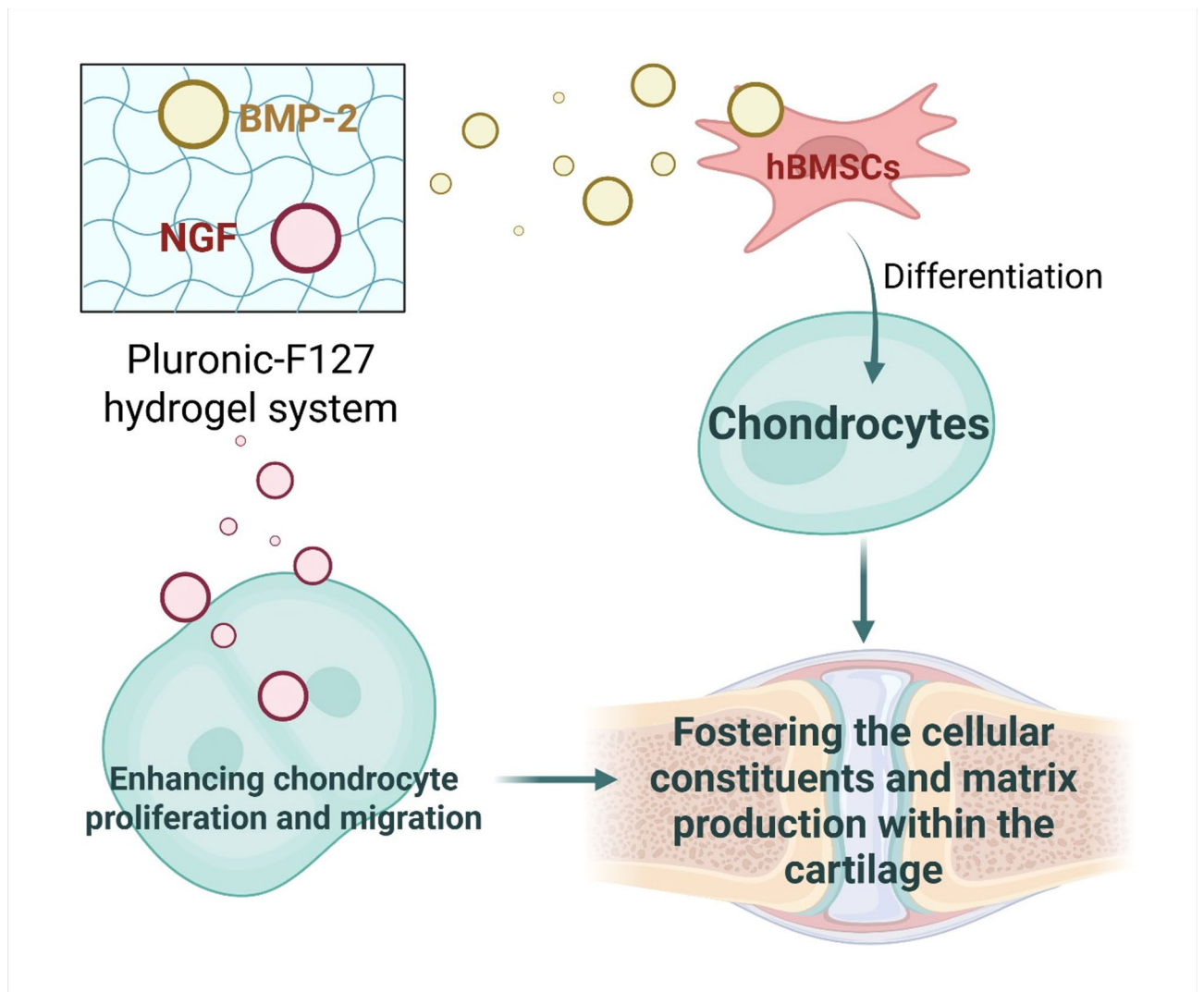


Fig. 7. The mechanism of NGF/BMP-2@Pluronic-F127 co-delivery system. Co-delivery of NGF and BMP-2 via a thermosensitive Pluronic-F127 hydrogel creates a bioactive microenvironment that synergistically promotes cartilage repair. BMP-2 induces chondrogenic differentiation of hBMSCs, while NGF enhances chondrocyte proliferation and migration. The sustained and localized release of both factors facilitates cellular proliferation, migration, and extracellular matrix deposition, ultimately promoting the formation of hyaline-like cartilage.

Data availability

Datasets generated during the current study are available from the corresponding author on reasonable request.

Received: 16 October 2024; Accepted: 14 August 2025

Published online: 29 September 2025

References

1. Jun, Y. et al. Transforming growth factor-beta1 promotes articular cartilage repair through canonical Smad and Hippo pathways in bone mesenchymal stem cells. *Life Sci.* **192** (0). <https://doi.org/10.1016/j.lfs.2017.11.028> (2017).
2. Daisuke, T., Hideki, Y. & Takashi, K. Cartilage and bone destruction in arthritis: pathogenesis and treatment strategy: a literature review. *Cells* **8** (8). <https://doi.org/10.3390/cells8080818> (2019).
3. Matsushita, T. et al. Surgical treatment of cartilage lesions in the knee: a narrative review. *J. Joint Surg. Res.* **1** (1), 70–79 (2023).
4. Hinckel, B. B. et al. Algorithm for treatment of focal cartilage defects of the knee: classic and new procedures. *Cartilage* **13** (1 suppl), 473S–495S (2021).
5. Brittberg, M. New frontiers for cartilage repair, joint preservation and prevention. *J. Cartil. Joint Preservation.* **2** (2), 100060 (2022).
6. Madry, H., Grün, U. W. & Knutsen, G. Cartilage repair and joint preservation: medical and surgical treatment options. *Deutsches Ärzteblatt Int.* **108** (40), 669 (2011).
7. Solanki, K., Shanmugasundaram, S., Shetty, N. & Kim, S. J. Articular cartilage repair & joint preservation: A review of the current status of biological approach. *J. Clin. Orthop. Trauma.* **22**, 101602 (2021).

8. Medvedeva, E. V. et al. Repair of damaged articular cartilage: current approaches and future directions. *Int. J. Mol. Sci.* **19** (8), 2366 (2018).
9. Liu, Y., Zhou, G. & Cao, Y. Recent progress in cartilage tissue engineering—our experience and future directions. *Engineering* **3** (1), 28–35 (2017).
10. Stampoulzis, T., Karami, P. & Pioletti, D. P. Thoughts on cartilage tissue engineering: A 21st century perspective. *Curr. Res. Translational Med.* **69** (3), 103299 (2021).
11. Wasyleczko, M., Sikorska, W. & Chwojnowski, A. Review of synthetic and hybrid scaffolds in cartilage tissue engineering. *Membranes* **10** (11), 348 (2020).
12. Xinhui, W., Yuan, M., Feng, L. & Qiang, C. The diversified hydrogels for biomedical applications and their imperative roles in tissue regeneration. *Biomater. Sci.* **11** (8). <https://doi.org/10.1039/d2bm01486f> (2023).
13. Ngadimin, K. D., Stokes, A., Gentile, P. & Ferreira, A. M. Biomimetic hydrogels designed for cartilage tissue engineering. *Biomaterials Sci.* **9** (12), 4246–4259 (2021).
14. Juncheng, G., Yijun, Y., Yang, X., Xueyi, G. & Shufang, Z. Pluronic F127 hydrogel-loaded extracellular vesicles from adipose-derived mesenchymal stem cells promote tracheal cartilage regeneration via SCNN1B delivery. *Nanomedicine* **58** (0). <https://doi.org/10.1016/j.nano.2024.102748> (2024).
15. Hafezi, M., Nouri Khorasani, S., Zare, M., Esmaeely Neisiany, R. & Davoodi, P. Advanced hydrogels for cartilage tissue engineering: recent progress and future directions. *Polymers* **13** (23), 4199 (2021).
16. Kwon, H., Paschos, N. K., Hu, J. C. & Athanasiou, K. Articular cartilage tissue engineering: the role of signaling molecules. *Cell. Mol. Life Sci.* **73**, 1173–1194 (2016).
17. Thielen, N. G., Van Der Kraan, P. M. & Van Caam A. P. TGF β /BMP signaling pathway in cartilage homeostasis. *Cells* **8** (9), 969 (2019).
18. Shen, B., Wei, A., Tao, H., Diwan, A. D. & Ma, D. D. BMP-2 enhances TGF- β 3-mediated chondrogenic differentiation of human bone marrow multipotent mesenchymal stromal cells in alginate bead culture. *Tissue Eng. Part A*. **15** (6), 1311–1320 (2009).
19. Hoffmann, A. & Gross, G. BMP signaling pathways in cartilage and bone formation. *Crit. Rev. Eukaryot. Gene Expr.* **11** (1–3), 23–45 (2001).
20. Censi, R., Dubbini, A. & Matricardi, P. Bioactive hydrogel scaffolds-advances in cartilage regeneration through controlled drug delivery. *Curr. Pharm. Design.* **21** (12), 1545–1555 (2015).
21. Tateiwa, D. et al. A novel BMP-2-loaded hydroxyapatite/beta-tricalcium phosphate microsphere/hydrogel composite for bone regeneration. *Sci. Rep.* **11** (1), 16924 (2021).
22. Tran, H. D., Park, K. D., Ching, Y. C., Huynh, C. & Nguyen, D. H. A comprehensive review on polymeric hydrogel and its composite: matrices of choice for bone and cartilage tissue engineering. *J. Ind. Eng. Chem.* **89**, 58–82 (2020).
23. Amiryaghoubi, N., Fathi, M., Barar, J. & Omid, Y. Hydrogel-based scaffolds for bone and cartilage tissue engineering and regeneration. *Reactive Funct. Polym.* **177**, 105313 (2022).
24. Zhang, Z. et al. Engineered sensory nerve guides Self-adaptive bone healing via NGF-TrkA signaling pathway. *Adv. Sci.* **10** (10), 2206155 (2023).
25. Yang, X. et al. Nerve growth factor promotes osteogenic differentiation of MC3T3-E1 cells via BMP-2/Smads pathway. *Annals Anatomy-Anatomischer Anzeiger.* **239**, 151819 (2022).
26. Zhang, Y., Zhao, X., Ge, D., Huang, Y. & Yao, Q. The impact and mechanism of nerve injury on bone metabolism. *Biochem. Biophys. Res. Commun.* **704**, 149699. <https://doi.org/10.1016/j.bbrc.2024.149699> (2024).
27. Rivera, K. O. et al. Local injections of β -NGF accelerates endochondral fracture repair by promoting cartilage to bone conversion. *Sci. Rep.* **10** (1), 22241 (2020).
28. Zhang, R., Liang, Y. & Wei, S. The expressions of NGF and VEGF in the fracture tissues are closely associated with accelerated clavicle fracture healing in patients with traumatic brain injury. *Ther. Clin. Risk Manag.* **14**, 2315–2322. <https://doi.org/10.2147/T.CRM.S182325> (2018).
29. Ye, J., Huang, B. & Gong, P. Nerve growth factor-chondroitin sulfate/hydroxyapatite-coating composite implant induces early osseointegration and nerve regeneration of peri-implant tissues in beagle dogs. *J. Orthop. Surg. Res.* **16**, 1–12 (2021).
30. Smith, P. K. et al. Measurement of protein using bicinchoninic acid. *Anal. Biochem.* **150** (1), 76–85. [https://doi.org/10.1016/0003-2697\(85\)90442-7](https://doi.org/10.1016/0003-2697(85)90442-7) (1985).
31. Orimo, A. et al. Successful germ-line transmission of chimeras generated by coculture aggregation with J1 ES cells and eight-cell embryos. *Anal. Biochem.* **269** (1), 204–207. <https://doi.org/10.1006/abio.1999.4007> (1999).
32. Farndale, R. W., Buttle, D. J. & Barrett, A. J. Improved quantitation and discrimination of sulphated glycosaminoglycans by use of dimethylmethylene blue. *Biochim. Biophys. Acta.* **883** (2), 173–177. [https://doi.org/10.1016/0304-4165\(86\)90306-5](https://doi.org/10.1016/0304-4165(86)90306-5) (1986).
33. Garcia-Couce, J. et al. Chitosan/Pluronic F127 thermosensitive hydrogel as an injectable dexamethasone delivery carrier. *Gels* **8** (1). <https://doi.org/10.3390/gels8010044> (2022).
34. Guo, J., Yang, Y., Xiang, Y., Guo, X. & Zhang, S. Pluronic F127 hydrogel-loaded extracellular vesicles from adipose-derived mesenchymal stem cells promote tracheal cartilage regeneration via SCNN1B delivery. *Nanomedicine* **58**, 102748. <https://doi.org/10.1016/j.nano.2024.102748> (2024).
35. Sarah, A. Microenvironmental regulation of chondrocyte plasticity in endochondral repair—a new frontier for developmental engineering. *Front. Bioeng. Biotechnol.* **6** (0). <https://doi.org/10.3389/fbioe.2018.00058> (2018).
36. Wei-Hui, C., Chuan-Qing, M., Li-Li, Z. & Joo, L. Beta-nerve growth factor promotes neurogenesis and angiogenesis during the repair of bone defects. *Neural Regen Res.* **10** (7). <https://doi.org/10.4103/1673-5374.160114> (2015).
37. Zheng, J. et al. Stepwise proliferation and chondrogenic differentiation of mesenchymal stem cells in collagen sponges under different microenvironments. *Int. J. Mol. Sci.* **23** (12). <https://doi.org/10.3390/ijms23126406> (2022).
38. Wang, M., Lian, J., Ye, M. & An, B. Pain mediator NGF improves chondrocyte extracellular matrix synthesis via PI3K/AKT pathway. *J. Orthop. Surg. Res.* **20** (1), 207. <https://doi.org/10.1186/s13018-025-05503-x> (2025).
39. Franco, R. et al. Microtissue culture provides clarity on the relative chondrogenic and hypertrophic response of bone-marrow-derived stromal cells to TGF-beta1, BMP-2, and GDF-5. *Cells* **13** (1). <https://doi.org/10.3390/cells13010037> (2023).
40. Xianfang, J. et al. Therapy for cartilage defects: functional ectopic cartilage constructed by cartilage-simulating collagen, chondroitin sulfate and hyaluronic acid (CCH) hybrid hydrogel with allogeneic chondrocytes. *Biomater. Sci.* **6** (6). <https://doi.org/10.1039/c8bm00354h> (2018).

Author contributions

Y. H., B. S., YY. L., GS. Z., and K. S designed the study, performed investigations, and collected all data. Y. H. wrote the draft of the main manuscript text. B. S. revised the manuscript. All authors reviewed the manuscript and approved the manuscript for submission.

Funding

The present study was supported by the 2023 Annual Fujian Provincial Joint Fund for Science and Technology Innovation “Double High” Project (No. 2023Y9058).

Declarations

Competing interests

The authors declare no competing interests.

Additional information

Supplementary Information The online version contains supplementary material available at <https://doi.org/10.1038/s41598-025-16308-7>.

Correspondence and requests for materials should be addressed to B.S.

Reprints and permissions information is available at www.nature.com/reprints.

Publisher's note Springer Nature remains neutral with regard to jurisdictional claims in published maps and institutional affiliations.

Open Access This article is licensed under a Creative Commons Attribution-NonCommercial-NoDerivatives 4.0 International License, which permits any non-commercial use, sharing, distribution and reproduction in any medium or format, as long as you give appropriate credit to the original author(s) and the source, provide a link to the Creative Commons licence, and indicate if you modified the licensed material. You do not have permission under this licence to share adapted material derived from this article or parts of it. The images or other third party material in this article are included in the article's Creative Commons licence, unless indicated otherwise in a credit line to the material. If material is not included in the article's Creative Commons licence and your intended use is not permitted by statutory regulation or exceeds the permitted use, you will need to obtain permission directly from the copyright holder. To view a copy of this licence, visit <http://creativecommons.org/licenses/by-nc-nd/4.0/>.

© The Author(s) 2025